batteries

Article

Synthesis of Three Ternary NiPP@PDA@DTA by Bridging Polydopamine and Its Flame Retardancy in Epoxy Resin

Wenxin Zhu [1], Huiyu Chai [1], Yue Lu [1], Wang Zhan [1,2] and Qinghong Kong [1,2,*]

[1] School of the Environment and Safety Engineering, Jiangsu University, Zhenjiang 212013, China; 2212209029@stmail.ujs.edu.cn (W.Z.); 2212009026@stmail.ujs.edu.cn (H.C.); 3220904008@stmail.ujs.edu.cn (Y.L.); zhanwang@ujs.edu.cn (W.Z.)
[2] School of Emergency Management, Jiangsu University, Zhenjiang 212013, China
* Correspondence: kongqh@ujs.edu.cn

Abstract: Epoxy resin (EP) is an indispensable packaging material for batteries. Excellent thermal and flame-retardant properties of EP can ensure the safety performance of batteries. To solve the low-efficiency flame retardant of EP, nickel phenyl phosphate (NiPP) was synthesized and its surface was modified by polymerization of dopamine (PDA). [3-(hydroxy-phenyl-methylidene) imimine] triazole (DTA) was synthesized using 9,10-dihydro-9-oxygen-10-phosphophene-10-oxide (DOPO), 3-amino-1,2,4-triazole and p-hydroxybenzaldehyde. The hybrid flame retardance NiPP@PDA@DTA was further synthesized by self-assembly between the negative charge on the surface of DTA and the positive charge on the surface of modified NiPP@PDA. Then, NiPP@PDA@DTA was added to EP to prepare EP/NiPP@PDA@DTA composites. The results showed that the incorporation of NiPP@PDA@DTA promoted the residual yield at high temperatures. Furthermore, EP composites showed excellent flame retardancy when NiPP@PDA@DTA was added. The EP/4 wt% NiPP@PDA@DTA composites can reach UL-94 V0 grade with a limit oxygen index (LOI) of 33.7%. While the heat release rate (HRR), total release rate (THR), CO_2 production (CO_2P) and total smoke release (TSR) of EP/4 wt% NiPP@PDA@DTA composites decreased by 16.9%, 30.8%, 16.9% and 27.7% compared with those of EP. These improvements are mainly due to the excellent catalytic carbonization performance of Ni metal and P compounds. The azazole and phosphaphenanthrene groups have the effects of dilution quenching in the gas phase and cross-linking network blocking, as well as enhanced blowing-out effects.

Keywords: phenyl metal phosphate; azazole; DOPO; packaging safety; flame retardant

Citation: Zhu, W.; Chai, H.; Lu, Y.; Zhan, W.; Kong, Q. Synthesis of Three Ternary NiPP@PDA@DTA by Bridging Polydopamine and Its Flame Retardancy in Epoxy Resin. *Batteries* **2024**, *10*, 428. https://doi.org/10.3390/batteries10120428

Academic Editor: Marco Giorgetti

Received: 18 October 2024
Revised: 26 November 2024
Accepted: 29 November 2024
Published: 3 December 2024

1. Introduction

EP is used in the field of power batteries because of their good insulation, chemical resistance and high strength, which helps to improve battery performance and enhance safety. With the continuous progress of technology, the application of epoxy resin in the field of power batteries will be broader [1,2]. However, the inflammability of EP generates potential fire hazards and greatly limits its application areas that require high fire safety performance [3,4]. Thus, it is necessary to improve the fire retardancy of EP [5,6].

Phosphates have attracted great interest as flame retardants of polymers. Metal organophosphates have been designed and prepared. Their effectiveness as flame retardants has been proven [7]. The PHRR value of PS composites was reduced by 39.8% when 5 wt% layered aluminum organic phosphate was added [8]. In addition, the heat release of polymer composites was significantly decreased by the homogeneous dispersion of metal–organic organophosphates with different morphologies. Layered cerium phenyl phosphate [9], rod-like phosphate-containing metal complexes [10], layered lanthanum phenyl phosphate [11], layered copper phenyl phosphate [12] and phosphorylenimide zinc [13]. The yield increases significantly due to the dehydrogenation of phosphorus compounds and the catalytic action of metal compounds in the process of carbonization [14].

The synergism between phosphorus and metal compounds promotes the cross-linking of the main chain and the suppression of flame propagation in the gas phase [15,16].

Dopamine (DA) can be self-polymerized to produce a polydopamine (PDA) coating that adheres to the surface of metals, metal oxides, graphene and hydrophobic polymers [17]. Moreover, PDA can provide abundant active groups for further modification. When the nano-hybrid MoS_2-PDA@$Ni(OH)_2$ was introduced into the PLA matrix, the yield was increased by 7.2% and the PHRR was decreased by 21.7% [18]. The introduction of h-BN@PDA@SnO_2 nanohybrids can improve the dispersed state of h-BN in the EP matrix. The thermal performance and flame retardant of EP/BN@PDA@SnO_2 composites obviously improved [19]. On the other hand, the PDA layer has amphoteric properties due to the amino and phenolic hydroxyl groups in the PDA structure [20]. Specifically, the PDA layer has a positive charge under acidic conditions. The PDA layer shows opposite characteristics under alkaline conditions [21]. Inspired by these, it is believed that the formation of a PDA layer on a metallic phenyl phosphate surface provides further functionalization of hybrid nanosheets.

In recent years, 9, 10-dihydro-9-oxygen-10-phosphophene-10-oxide (DOPO) has attracted wide attention because of its remarkable flame retardancy [22]. The active P-H bond in DOPO can react with amino, carbonyl, epoxy group and other electron-deficient compounds to form DOPO derivatives, which have remarkably improved flame retardancy because of the multiple element synergistic action [23]. Among these, DOPO derivatives containing nitrogen heterocyclics like triazine, maleimide, phosphazene and triazine-trione have received extensive attention for suitable thermal stability and high flame-retardant activity [24]. EP composites reached a UL-94 V0 rating with the incorporation of 6 wt% flame retardant with phosphaphenanthrene group and tetrazole ring [25].

Based on the above review, we attempted to combine the excellent catalytic performance of Ni and P compounds, the gas-phase dilution quenching effect and the cross-linking network barrier effect of the azole group and the phosphaphenanthrene group, and the reinforcing effect of the blow-out effect. Schiff base (DTA) was synthesized from p-hydroxybenzaldehyde, 3-amino-1,2,4-triazole and DOPO. Then, a positively charged PDA layer was formed on the surface of nickel phenyl phosphate (NiPP) under acidic conditions. And the hybrid nanosheet NiPP@PDA@DTA was prepared by in situ synthesis of negatively charged azolium schiff base layer on the surface. The EP/NiPP@PDA@DTA composites were prepared and their thermal properties and flame-retardant properties were studied.

2. Materials and Methods

2.1. Materials

P-hydroxybenzaldehyde ($C7H_6O_2$), 3-amino 1,2,4-triazole ($C_2H_4N_4$), Tris–HCl buffer and dopamine (DA) were bought from Macklin Co., Ltd. (Shanghai, China). Phenylphosphonic acid (>98%) was acquired from TCl Chemicals Company (Huizhou, China). Polyvinylpyrrolidone (PVP), hexamethyltetramine ($C_6H_{12}N_4$), nickel nitrate hexahydrate ($Ni(NO_3)_2{\cdot}6H_2O$), 9,10-dihydro-9-oxygen-10-phospha-phenanthrene-10-oxide (DOPO), ethylene glycol ($(CH_2OH)_2$), ethanol (CH_3CH_2OH), HCl and diaminodiphenylmethane (DDM) were acquired from Sinopharm Chemical Reagent Co., Ltd. (Shanghai China). EP (NPEL128) was purchased from Nanya Electronic Materials Co., Ltd. (Kunshan, China).

2.2. Synthesis of NiPP@PDA@DTA

The synthesis graph of NiPP@PDA@DTA is shown in Figure 1. The NiPP was produced in the lab based on the previous literature. NiPP was synthesized according to the procedure given by Kong et al. [7]. An amount of 0.50 g NiPP was dispersed in 80 mL deionized water and 30 mL ethanol by ultrasonic for 30 min. Then, 0.20 g of DA and 0.32 g of Tris–HCl buffer were added to the above NiPP suspension with an 8.5 PH value, slowly

stirred and reacted at 30 °C for 24 h. Finally, the product of NiPP@PDA is obtained by filtration and washed with deionized water.

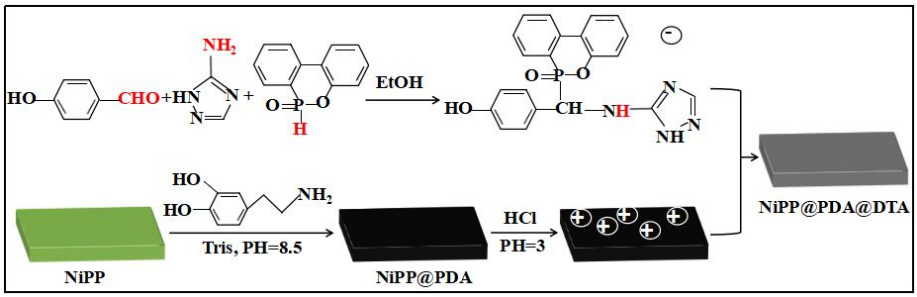

Figure 1. Schematic representation of the synthesis of NiPP@PDA@DTA.

Amounts of 1.00 g NiPP@PDA, 1 mL of hydrochloric acid and 60 mL of ethanol were added to a 500 mL three-port flask with a stirring and reflux device for 30 min, and then 1.68 g 3-amino-1,2,4-triazole was added. Next, 2.40 g p-hydroxybenzaldehyde was slowly added to the mixture and stirred for 2 h at 80 °C. Then, 4.32 g DOPO was added and reacted for 12 h. The product was washed with ethanol and vacuum dried, which was labeled as NiPP@PDA@DTA.

2.3. Preparation of EP/NiPP@PDA@DTA Composites

EP composites were prepared as follows: An amount of flame retardant and an appropriate amount of EP were put on a three-roll grinder and fully rotated by shear force for 30 min. The above mixtures were collected in a beaker and stirred at 90 °C. DDM (the mass ratio of EP to DDM is 4:1) was added to the EP mixtures. The above mixture was poured into the preheated mold and cured at 100 °C for 2 h. It was cared for at 110 °C, 130 °C and 150 °C for 2 h, respectively. The content of the EP composite is shown in Table 1.

Table 1. Ingredients of EP composites.

Samples	Components				
	EP + DDM (wt%)	**NiPP@PDA@DTA (wt%)**	**NiPP (wt%)**	**NiPP@PDA (wt%)**	**DTA (wt%)**
EP	100.0	0	0	0	0
EP/2 wt%NiPP@PDA@DTA	98	2	0	0	0
EP/4 wt%NiPP@PDA@DTA	96	4	0	0	0
EP/6 wt%NiPP@PDA@DTA	94	6	0	0	0
EP/4 wt%NiPP	96	0	4	0	0
EP/4 wt%NiPP@PDA	96	0	0	4	0
EP/4 wt%DTA	96	0	0	0	4

2.4. Characterization

X-ray diffraction (XRD) patterns of NiPP@PDA@DTA and NiPP@PDA were measured with a MAX-Rb instrument produced by Rigaku Co., Ltd. (Tokyo, Japan), which had a scanning speed of 5 °/min. Fourier transform infrared (FTIR) spectra were obtained with a 6700 spectrometer produced by Nicolet Instruments Co., Ltd. (Madison, WI, USA). Its spectral frequency range was 400–4000 Hz/cm. Scanning electron microscopy (SEM) of NiPP@PDA@DTA and NiPP@PDA was used by JSM-7001F, and gold spraying was required before testing. The nuclear magnetic resonance (NMR) test was used with the Bruker AVANCE II 400 MHz NMR (Bruker, Germany).

Vertical combustion tests were tested by CZF-1 coming from Jiangning Analytical Instrument Co., Ltd. (Nanjing, China). The spline size was 130 × 13 × 3.2 mm^3. The test standard was in accordance with ASTM D3801-20a [26]. The LOI was tested by the JF-3 oxygen index instrument produced by Jiangning Analytical Instrument Co., Ltd. The

spline size was 130 × 6.5 × 3.2 mm^3 and the test standard was in accordance with ASTM D2863-23 [27]. TGA was conducted using the TA Q50 thermal analyzer (TA Instrument Company, New Castle, DE, USA) at the ramp rate of 10 °C/min in N_2 flow. The cone calorimeter test (CCT) of EP and EP composites was used with the FTT cone calorimeter according to ISO 5660-1 at a heat flux of 35 kW/m^2 [28].

3. Results

3.1. Structural Analysis of NiPP@PDA@DTA

XRD patterns (Figure 2a) show that the diffraction peaks of NiPP appear at 6.2°, 12.2° and 17.0° [7]. The diffraction peak positions of NiPP@PDA are consistent with those of NiPP. The diffraction peaks around 8.5°, 11.5°, 16.1°, 22.6° and 26.1° are the presented spectrum of DTA [29]. Ultimately, the diffraction peaks at 6.2° belonged to NiPP and 8.5° belonged to DTA, which confirms the successful synthesis of NiPP@PDA@DTA. The 010 plane peak is weaker than that of NiPP, which is caused by surface coating.

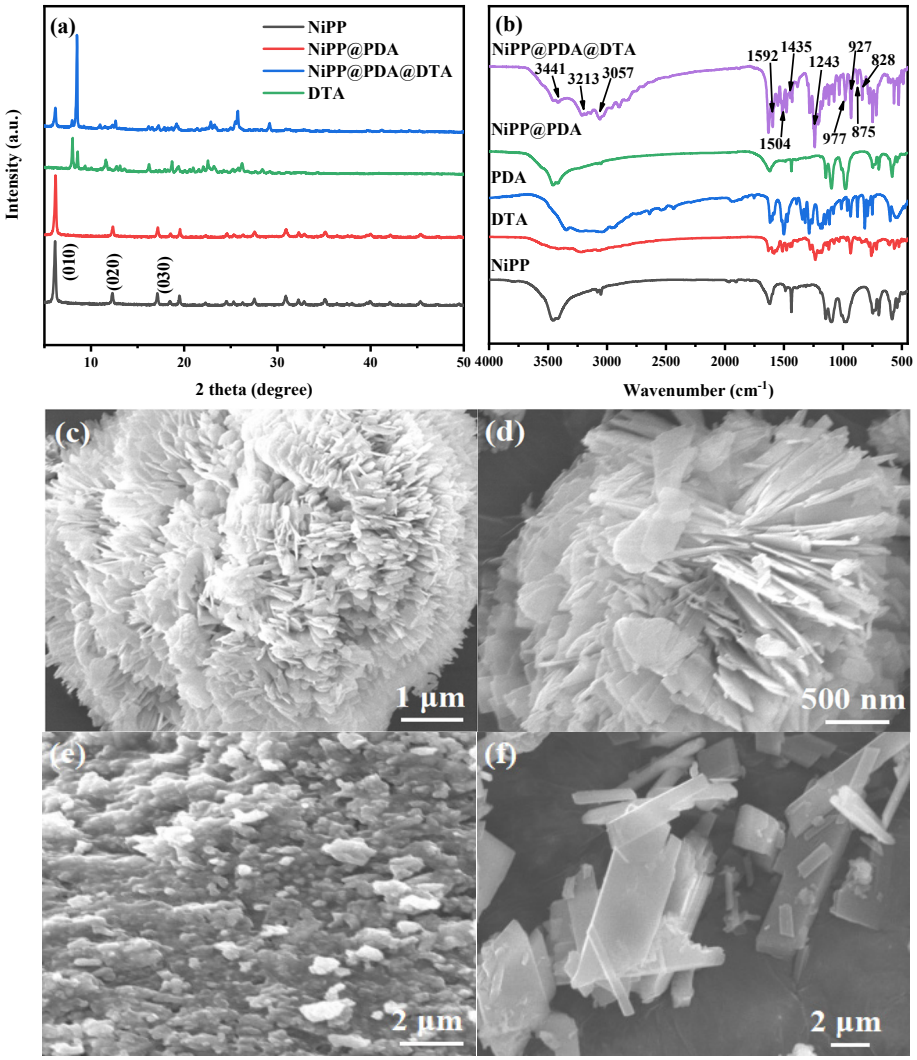

Figure 2. (**a**) XRD patterns of NiPP, NiPP@PDA, NiPP@PDA@DTA and DTA; (**b**) FTIR curves of NiPP, NiPP@PDA, NiPP@PDA@DTA, PDA and DTA; (**c**) SEM images of NiPP; (**d**) SEM image of NiPP@PDA; (**e**) SEM image of DTA; (**f**) SEM image of NiPP@PDA@DTA.

The FTIR spectra (Figure 2b) of relevant flame retardants reveal that the characteristic absorption peak at 3441 cm^{-1} belongs to the stretching vibration of -OH in adsorbed water. The characteristic absorption peak at 3057 cm^{-1} corresponds to the stretching vibration of the C-H bond [30]. The characteristic absorption peak at 1435 cm^{-1} was assigned to the

stretching vibration of the C=C bond. There is a peak of 1035 cm^{-1} corresponding to the stretching vibration of the Ni-O-P bond. The characteristic absorption peak at 977 cm^{-1} is the stretching vibration of the P-O bond [31]. The results showed that the above analysis corresponds to the molecular structure of NiPP. However, the specific functional groups of the polydopamine layer on the NiPP surface were not observed due to its low signal intensity and the mask of -OH in NiPP. The characteristic absorption peaks of 3213 cm^{-1} (N-H), 1592 cm^{-1} (C=N), 1504 cm^{-1} (P-Ph), 1243 cm^{-1} and 926 cm^{-1} (P-O-Ph) and 875 cm^{-1} and 828 cm^{-1} (C-H bonds in the structure of phosphaphenanthrene) are detected, which indicates the successful synthesis of NiPP@PDA@DTA [32].

Figure 2c–f give the SEM images of related flame retardants. The results showed that NiPP was a flower-like structure assembled from nanosheets. The microstructure of NiPP@PDA was similar to that of NiPP. The diameter of the sphere was increased and the agglomeration phenomenon was alleviated, which was due to the attenuated interaction force between the nanosheets. It is very important that the lamellar structure of NiPP@PDA@DTA ternary composites is scattered.

The peak of the H-NMR spectrum (Figure 3a) of DTA at 11.80 ppm corresponds to the hydrogen atom (H) in the triazole ring. The peak at 9.46 ppm belongs to the hydrogen atom (Ha) of the phenol hydroxyl group [33]. The peaks at a range of 5.07–5.44 ppm are assigned to the hydrogen atom (Hc) in methine groups. The signal peak of the hydrogen atom (Hd) on the imino attached to the triazole ring appeared at 8.13–8.26 ppm, while the signal peak of the hydrogen atom (Hb) on the aromatic ring was observed at 7.05–8.27 ppm [34]. Taken together, it confirms the expected chemical structure of DTA.

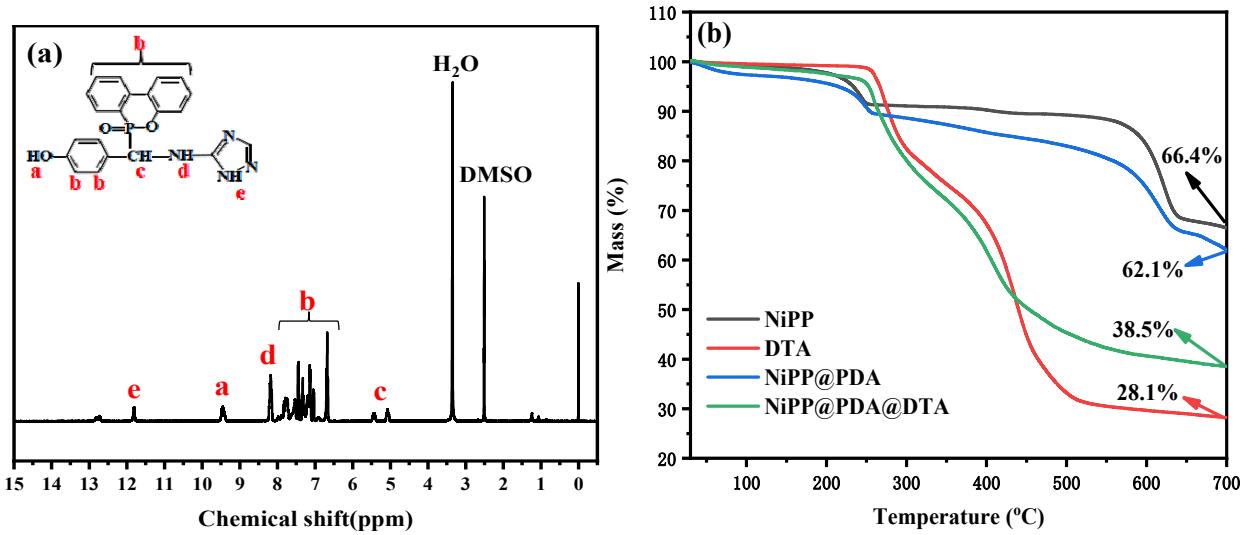

Figure 3. (**a**) NMR spectra of DTA; (**b**) TGA curves of NiPP, DTA, NiPP@PDA and NiPP@PDA@DTA.

Figure 3b shows the TGA curves of NiPP, DTA, NiPP@PDA and NiPP@PDA@DTA. The weight loss of NiPP was about 7.3% below 250 °C, which was the desorption of adsorbed water and glycol. The thermal degradation of the benzene ring of the NiPP occurred after 550 °C. The mass loss of NiPP was 26.3%, indicating that NiPP has high thermal stability [7]. The thermal degradation process of NiPP@PDA was similar to that of NiPP after PDA modification, and the residual amount is 62.1%. DTA begins to degrade at about 260 °C. The process of degradation of DTA underwent two major decomposition processes of DOPO and triazole rings from 260 to 500 °C [35]. The residual amount of DTA at 700 °C was 28.1%. The decomposition process of NiPP@PDA@DTA is similar to that of DTA due to the content of NiPP. The main thermal decomposition stage occurred between 260 °C and 550 °C, which was consistent with the main pyrolysis temperature of EP, so it was more suitable as a flame retardant for EP. The residual amount of NiPP@PDA@DTA at

700 °C was 38.5%, which was attributed to the P-C and O-P-O bonds in DTA being less thermally stable than ordinary C-C bonds [36].

3.2. Thermal Properties of EP/NiPP@PDA@DTA Composites

To observe the dispersion of NiPP@PDA@DTA in EP, the fracture morphologies of EP/4%NiPP and EP/4%NiPP@PDA@DTA composites were tested by SEM, as shown in Figure 4. NiPP were well dispersed in EP. There was also a small amount of agglomeration in Figure 4a. Figure 4b showed that NiPP@PDA@DTA was evenly dispersed on the surface of the EP matrix, which indicated that NiPP@PDA@DTA has good compatibility with EP.

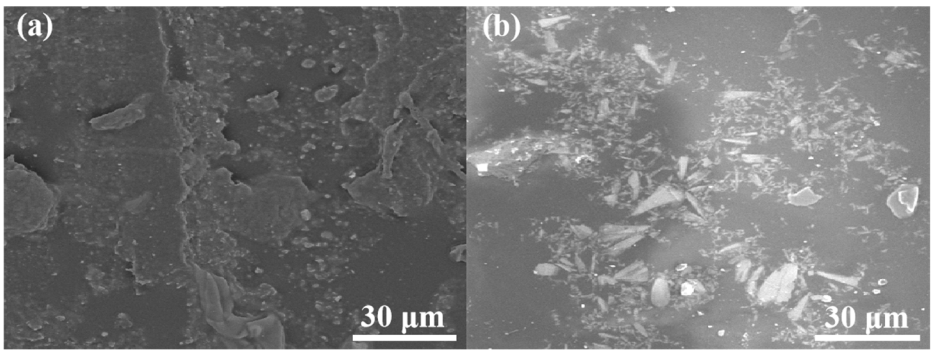

Figure 4. (**a**) SEM image of EP/4% NiPP composites, (**b**) SEM image of EP/NiPP@PDA@DTA composites.

TGA and DTG curves of EP and EP composites are shown in Figure 5. And specific values are listed in Table 2. The initial decomposition temperature ($T_{5\%}$) and temperature at the maximum pyrolysis rate (T_{max}) of EP were 353 °C and 369 °C. When 4 wt% NiPP@PDA@DTA was added, the NiPP@PDA@DTA promoted the decomposition of EP at low temperatures. The residue of Ep/4 wt% NiPP@PDA@DTA at 700 °C was increased to 18.2%, which was higher than those of EP (13.5%), EP/4 wt% NiPP@PDA (16.5%), EP/4 wt% PDA (17.0%) and EP/4 wt% NiPP (16.5%). The excellent thermal performance of EP/NiPP@PDA@DTA composites was attributed to the excellent catalytic performance of NiPP@PDA and the gas-phase dilution effect of triazole and phosphoheterophosphoric groups of DTA [37]. The T_{max} of the composites was decreased from 365 °C to 360 °C with the addition of 2, 4, 6 NiPP@PDA@DTA. The residue content of the composites went to 16.3%, 18.2% and 18.8%, respectively, which may be attributed to the fact that the phosphoric acid group and Ni compounds generated by the partial degradation of NiPP@PDA@DTA promoted the formation of phosphorous-rich coke [38].

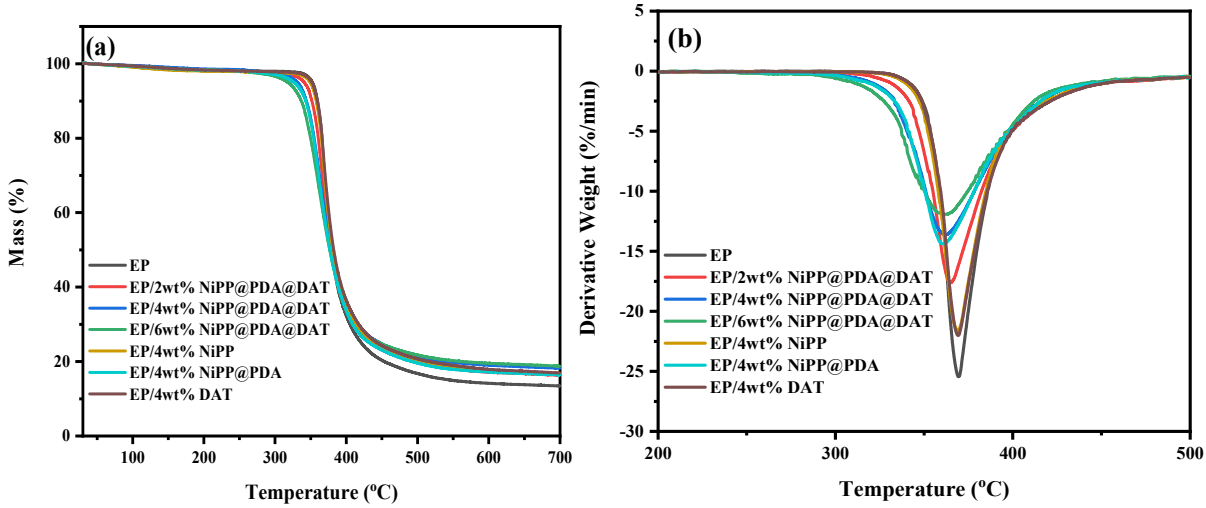

Figure 5. (**a**) TGA curves of pure EP and EP composites, (**b**) DTG curves of pure EP and EP composites.

Table 2. TGA results of pure EP and its composites.

Samples	$T_{5\%}$ (°C)	T_{max} (°C)	Residues (wt%, 700 °C)
EP	353	369	13.5
EP/2 wt%NiPP@PDA@DTA	340	365	16.3
EP/4 wt%NiPP@PDA@DTA	333	362	18.2
EP/6 wt%NiPP@PDA@DTA	319	362	18.8
EP/4 wt%NiPP	350	369	16.5
EP/4 wt%NiPP@PDA	328	361	16.5
EP/4 wt%DTA	354	369	17.0

3.3. Flame-Retardant Properties of EP/NiPP@PDA@DTA Composites

The LOI and UL-94 rating of EP/NiPP@PDA@DTA composites are shown in Table 3. The LOI of EP was 25.9%, and the vertical combustion test has no grade. When the content of NiPP or NiPP@PDA was only 4 wt%, the LOI of EP composites was slightly raised to 28.8% and the vertical combustion test is still no rating. However, EP/4 wt% DTA composites can reach UL-94 V1 grade, and the LOI goes up to 31.5%, which shows that the improvement of the flame retardancy of EP is great. Surprisingly, the vertical combustion result of EP composites can reach V0 grade by adding 4 and 6% NiPP@PDA@DTA. LOI is increased to 33.7% and 33.1%, respectively, indicating that the flame retardant of EP/NiPP@PDA@DTA composites was significantly improved compared with EP/DTA composites. The improvement in flame retardancy of EP/NiPP@PDA@DTA composites is attributed to phosphorus phase free radicals and Ni compounds in the decomposition of NiPP@PDA@DTA, which play the blocking catalysis effect [39].

Table 3. Vertical combustion and LOI results of EP and its composites.

Samples	LOI (vol%)	UL-94	
		$t_1 + t_2$ (s)	Rating
EP	25.9	>50	NR
EP/1 wt%NiPP@PDA@DTA	29.8	31.9	V-1
EP/2 wt%NiPP@PDA@DTA	30.6	23.2	V-1
EP/4 wt%NiPP@PDA@DTA	33.7	7.3	V-0
EP/6 wt%NiPP@PDA@DTA	33.1	8.9	V-0
EP/4 wt%NiPP	28.1	>50	NR
EP/4 wt%NiPP@PDA	28.8	>50	NR
EP/4 wt%DTA	31.5	18.6	V-1

To further analyze the combustion of EP composites, CCT was carried out. The heat release rate (HRR), smoke production rate (SPR), total smoke release (TSR) and CO_2 production (CO_2P) of EP composites are displayed in Figure 6 and Table 4. The PHRR value of EP was 1317 kW/m^2. The PHRR value of the composites was reduced to 1123 kW/m^2 and 1125 kW/m^2 by adding 4 wt% NiPP and DTA, respectively. It indicated that NiPP or DTA alone appropriately reduced the heat release from EP. The PHRR of EP composites with 2, 4 and 6 wt% NiPP@PDA@DTA declined to 1119, 1094 and 1021 kW/m^2, which decreased by 15.0%, 16.9% and 22.5% compared with EP, respectively. The reduction in PHRR of EP/NiPP@PDA@DTA composites may be due to the decomposition of NiPP@PDA@DTA to generate Ni-based oxides and phosphates, which promoted the formation of P-rich dense char layers. This char layer covered the polymer surface and prevented heat and mass transfer [40].

When 4 wt% of NiPP, NiPP@PDA and DTA were added, the THR of EP composites decreased to 97, 86 and 86 MJ/m^2, respectively, which were all lower than that of EP (104 MJ/m^2). The THR of EP/4 wt% NiPP@PDA@DTA composites (72 MJ/m^2), which was 30.8% lower than that of EP is the lowest in all of the EP composites. The reduction in the

THR value of EP/NiPP@PDA@DTA composites was attributed to the lamellar barrier and metal catalysis of NiPP and dilution quenching of DTA [41].

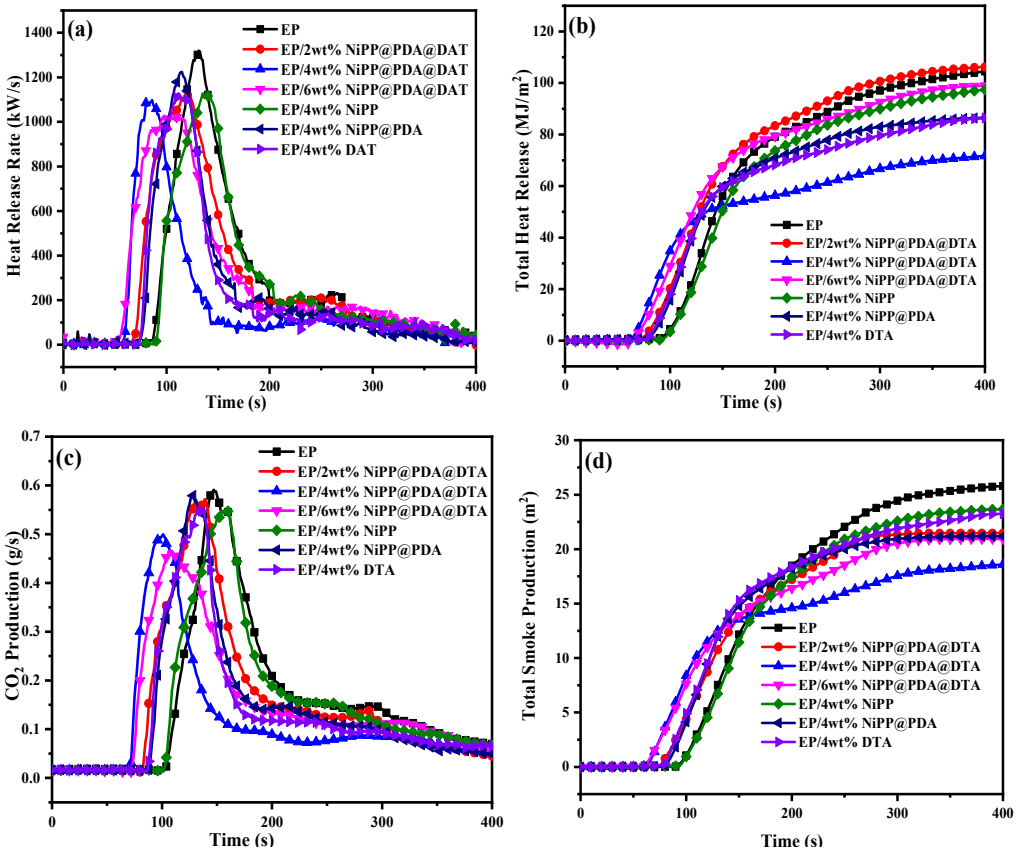

Figure 6. (**a**) HRR, (**b**) THR, (**c**) CO_2P and (**d**) TSP curves of pure EP and EP composites.

Table 4. CCT results of EP and EP composites.

Samples	TTI (s)	PHRR (kW/m^2)	THR (MJ/m^2)	CO_2P (g/s)	TSP (m^2)
EP	90	1317	104	0.59	26.0
EP/2 wt%NiPP@PDA@DTA	74	1119	106	0.56	21.4
EP/4 wt%NiPP@PDA@DTA	63	1094	72	0.49	18.8
EP/6 wt%NiPP@PDA@DTA	61	1021	99	0.46	20.9
EP/4 wt%NiPP	96	1123	97	0.54	23.7
EP/4 wt%NiPP@PDA	80	1221	86	0.58	21.1
EP/4 wt%DTA	79	1125	86	0.55	23.2

The CO_2P values of EP, EP/4 wt% NiPP, EP/4 wt% NiPP@PDA and EP/4 wt% DTA were 0.59, 0.54, 0.58 and 0.55 g/s, respectively, which indicated that the NiPP or DTA can appropriately reduce the release of CO_2 during the combustion of EP composites. However, the CO_2P value of EP/4 wt% NiPP@PDA@DTA composites was the lowest (0.49 g/s). When 2 and 6 wt% NiPP@PDA@DTA were added, the CO_2P value of EP composites declined to 0.56 and 0.46 g/s, which decreased by 5.1% and 22.0% compared with that of EP, respectively. The significant reduction of CO_2 in EP/NiPP@PDA@DTA composites is due to the fact that more residue is produced during the combustion of EP composites [42].

Generally speaking, the amount of smoke is an important index in fire escape. The TSP values of EP composites were 23.7, 21.1 and 23.2 m^2, respectively, adding 4 wt% NiPP, NiPP@PDA and DTA, which were all lower than that of EP (26.0 m^2). The TSP value of EP/4 wt% NiPP@PDA@DTA composites was further reduced to 18.8 m^2. The above results indicated that NiPP@PDA@DTA further reduced the formation of the volatile

gas-phase component and left more char in the condensed phase. It indicates that the addition of NiPP@PDA@DTA reduces the formation of volatile fractions in the gas phase and leaves more char in the condensed phase. Nevertheless, the TSP values of EP/6 wt%NiPP@PDA@DTA composites increased to 20.9 m^2, which may be because the excessive addition of NiPP@PDA@DTA made the composites exhibit more vapor flame-retardant effect, accelerating the release of quenching free radicals and non-flammable gases [43].

3.4. Flame-Retardant Mechanism of EP/NiPP@PDA@DTA Composites

Figure 7 is a schematic diagram of the flame-retardant mechanism. It can be inferred based on the thermal degradation and combustion of EP/NiPP@PDA@DTA composites. In the gas phase, NiPP and DTA release phosphorus free radicals in the pyrolysis process, which eliminates H and HO free radicals in the flame zone and interrupts the burning free radical chain reaction [44]. In addition, the cleavage of PDA and DTA can also produce nitrogen-containing compounds, which can be converted into non-flammable gases such as NH_3, N_2 and NO_2. The matrix combustion produced CO_2. These gases dilute oxygen and combustible gases, taking away the heat produced by combustion. The transition metal (Ni) plays a catalytic role in promoting the char formation of EP [45]. The residual phosphorus elements in the condensed phase can also be converted into phosphoric acid sources to promote the dehydration of epoxy groups. This dehydration carbonization can form a high-quality char layer that acts as a cavity barrier. When the amount of gas accumulated in the char layer exceeds the capacity of the char layer in the combustion process, the gas will be released centrally, which plays a blow-out effect, extinguishing the flame [46].

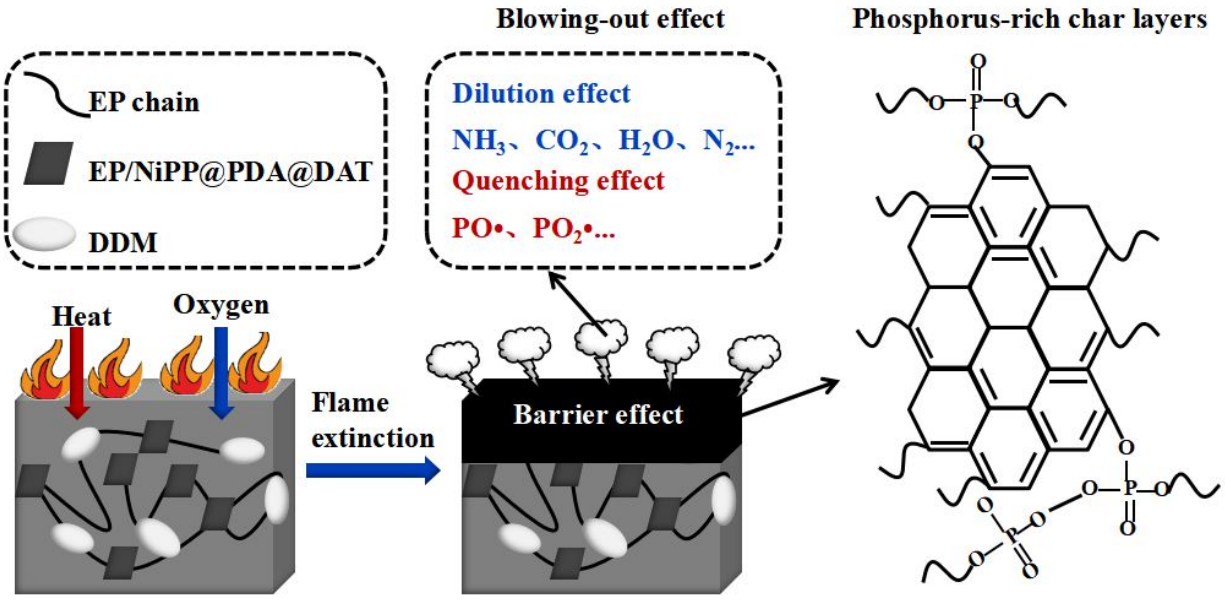

Figure 7. Schematic diagram of flame-retardant mechanism of NiPP@PDA@DTA in EP.

4. Conclusions

In summary, the hybrid flame-retardant NiPP@PDA@DTA was added to EP to prepare the composites, which can promote the cross-linked charring of EP in advance. The $T_{5\%}$ and T_{max} of EP composites in TGA were earlier. The flame retardant of EP was greatly improved with the addition of NiPP@PDA@DTA. EP/4 wt%NiPP@PDA@DTA composites reached the UL94 V-0 level, and the LOI value increased to 33.7%. The thermal and flame retardant properties of EP/NiPP@PDA@DTA composites were improved mainly due to the free radical quenching of the phosphorus phase, the dilution and endothermic effect of non-flammable gas, the catalytic effect of Ni metal and the dehydration of P phase into char, which had positive significance for fire rescue.

Author Contributions: Investigation, Y.L.; Resources, W.Z. (Wang Zhan); Writing—original draft, H.C.; Writing—review & editing, W.Z. (Wenxin Zhu); Project administration, Q.K. All authors have read and agreed to the published version of the manuscript.

Funding: This work was supported by the Natural Science Foundation of China (Grant No. 5220421), Jiangsu Collaborative Innovation Center of Technology and Material of Water Treatment, China and the Special Scientific Research Project of the School of Emergency Management of Jiangsu University (KY-B-06).

Data Availability Statement: Data are contained within the article.

Conflicts of Interest: The authors declare no conflict of interest.

References

1. Zhi, M.Y.; Yang, X.; Fan, R. A comprehensive review of reactive flame-retardant epoxy resin: Fundamentals, recent developments, and perspectives. *Polym. Degrad. Stab.* **2022**, *201*, 109976. [CrossRef]
2. Xiao, L.H.; Chen, X.; Yang, X.Y.; Sun, J.H.; Geng, J.X. Recent advances in polymer-based photothermal materials for biological applications. *ACS Appl. Polym. Mater.* **2020**, *2*, 4273–4288. [CrossRef]
3. Chen, M.; Yu, Y.; Ouyang, D.; Weng, J.; Zhao, L.; Wang, J.; Chen, Y. Research progress of enhancing battery safety with phase change materials. *Renew. Sustain. Energy Rev.* **2024**, *189*, 113921. [CrossRef]
4. Li, L.; Li, X.W.; Wan, S.B. High-efficiency flame-retardant epoxy resin using phosphoraphenanthrene/thiazole-based co-curing agent. *J. Therm. Anal. Calorim.* **2023**, *148*, 10115–10124. [CrossRef]
5. Madyaratri, E.W.; Ridho, M.R.; Aristri, M.A.; Lubis, M.A.; Iswanto, A.H.; Nawawi, D.S.; Antov, P.; Kristak, L.; Majlingová, A.; Fatriasari, W. Recent advances in the development of fire-resistant biocomposites—A review. *Polymers* **2022**, *14*, 362. [CrossRef] [PubMed]
6. Ouyang, D.; Chen, M.; Weng, J.; Wang, K.; Wang, J.; Wang, Z. Exploring the thermal stability of lithium-ion cells via accelerating rate calorimetry: A review. *J. Energy Chem.* **2023**, *81*, 543–573. [CrossRef]
7. Kong, Q.H.; Li, L.; Zhang, M.M. Improving the Thermal Stability and Flame Retardancy of Epoxy Resins by Lamellar Cobalt Potassium Pyrophosphate. *Polymers* **2022**, *14*, 4927. [CrossRef]
8. Hou, Y.B.; Hu, W.Z.; Hu, Y. Preparation of layered organic-inorganic aluminum phosphonate for enhancing fire safety of polystyrene. *Mater. Chem. Phys.* **2017**, *196*, 109–117. [CrossRef]
9. Kong, Q.H.; Wu, T.; Zhang, J.H.; Wang, D.Y. Simultaneously improving flame retardancy and dynamic mechanical properties of epoxy resin nanocomposites through layered copper phenylphosphate. *Compos. Sci. Technol.* **2018**, *154*, 136–144. [CrossRef]
10. Sai, T.; Ran, S.Y.; Guo, Z.H.; Yan, H.Q.; Zhang, Y.; Song, P.; Zhang, T.; Wang, H.; Fang, Z. Deposition growth of Zr-based MOFs on cerium phenylphosphonate lamella towards enhanced thermal stability and fire safety of polycarbonate. *Compos. Part B Eng.* **2020**, *197*, 108064. [CrossRef]
11. Liu, Y.; Cao, Z.H.; Zhang, Y.; Fang, Z.P. Synthesis of zinc N-morpholinomethylphosphonic acid and its application in high density polyethylene. *Fire Saf. J.* **2015**, *71*, 1–8. [CrossRef]
12. Ran, S.Y.; Ye, R.F.; Cai, Y.F.; Shen, Y.H.; He, Y.; Fang, Z.; Guo, Z. Synergistic flame retardant mechanism of lanthanum phenylphosphonate and decabromodiphenyl oxide in polycarbonate. *Polym. Compos.* **2019**, *40*, 986–999. [CrossRef]
13. Hu, P.; Li, W.; Huang, S.; Zhang, Z.; Liu, H.; Zhan, W.; Chen, M.; Kong, Q. Effect of Layered Aminovanadic Oxalate Phosphate on Flame Retardancy of Epoxy Resin. *Molecules* **2023**, *28*, 3322. [CrossRef]
14. Zhu, H.J.; Chen, Y.M.; Huang, S.; Wang, Y.; Yang, R.; Chai, H.; Zhu, F.; Kong, Q.; Zhang, Y.; Zhang, J. Suppressing fire hazard of poly (vinyl alcohol) based on $(NH_4)_2[VO(HPO_4)]_2(C_2O_4)\cdot 5H_2O$ with layered structure. *J. Appl. Polym. Sci.* **2021**, *138*, 51345. [CrossRef]
15. Ding, J.M.; Zhang, Y.; Zhang, X.; Kong, Q.H.; Zhang, J.H.; Liu, H. Improving the flame-retardant efficiency of layered double hydroxide with disodium phenylphosphate for epoxy resin. *J. Therm. Anal. Calorim.* **2020**, *140*, 149–156. [CrossRef]
16. Cui, J.F.; Zhang, Y.B.; Wang, L.R.; Liu, H.; Wang, N.N.; Yang, B.; Guo, J.; Tian, L. Phosphorus-containing Salen-Ni metal complexes enhancing the flame retardancy and smoke suppression of epoxy resin composites. *J. Appl. Polym. Sci.* **2020**, *137*, 48734. [CrossRef]
17. Yang, K.; Huang, X.Y.; He, J.L.; Jiang, P.K. Strawberry-like Core-Shell Ag@ Polydopamine@ $BaTiO_3$ hybrid nanoparticles for high-k polymer nanocomposites with high energy density and low dielectric loss. *Adv. Mater. Interfaces* **2015**, *2*, 1500361. [CrossRef]
18. Gao, R.; Wang, S.G.; Zhou, K.Q.; Qian, X.D. Mussel-inspired decoration of Ni $(OH)_2$ nanosheets on 2D MoS_2 towards enhancing thermal and flame retardancy properties of poly (lactic acid). *Polym. Adv. Technol.* **2019**, *30*, 879–888. [CrossRef]
19. Cai, W.; Guo, W.W.; Pan, Y.; Wang, J.L.; Mu, X.W.; Feng, X.; Yuan, B.; Wang, B.; Hu, Y. Polydopamine-bridged synthesis of ternary h-BN@ PDA@ SnO_2 as nanoenhancers for flame retardant and smoke suppression of epoxy composites. *Compos. Part A Appl. Sci. Manuf.* **2018**, *111*, 94–105. [CrossRef]

20. Li, Z.; Liu, L.J.; González, A.J.; Wang, D.Y. Bioinspired polydopamine-induced assembly of ultrafine Fe $(OH)_3$ nanoparticles on halloysite toward highly efficient fire retardancy of epoxy resin via an action of interfacial catalysis. *Polym. Chem.* **2017**, *8*, 3926–3936. [CrossRef]
21. Zheng, X.; Zhang, J.; Wang, J.; Qi, X.; Rosenholm, J.M.; Cai, K. Polydopamine coatings in confined nanopore space: Toward improved retention and release of hydrophilic cargo. *J. Phys. Chem. C* **2015**, *119*, 24512–24521. [CrossRef]
22. Jian, R.K.; Pang, F.Q.; Lin, Y.C.; Bai, W.B. Facile construction of lamellar-like phosphorus-based triazole-zinc complex for high-performance epoxy resins. *J. Colloid Interface Sci.* **2022**, *609*, 513–522. [CrossRef] [PubMed]
23. Sun, J.Z.; Zhang, D.H.; Shang, X.Y.; Tan, F.; Bao, D.M.; Qin, S.H. Flame-retardant properties and mechanism of LGF/PBT/DOPO-HQ-conjugated flame-retardant composites. *Front. Chem.* **2022**, *10*, 981579. [CrossRef]
24. Qian, L.J.; Qiu, Y.; Sun, N.; Xu, M.L.; Xu, G.Z.; Xin, F.; Chen, Y. Pyrolysis route of a novel flame retardant constructed by phosphaphenanthrene and triazine-trione groups and its flame-retardant effect on epoxy resin. *Polym. Degrad. Stab.* **2014**, *107*, 98–105. [CrossRef]
25. Wang, P.; Chen, L.; Xiao, H. Flame retardant effect and mechanism of a novel DOPO based tetrazole derivative on epoxy resin. *J. Anal. Appl. Pyrolysis* **2019**, *139*, 104–113. [CrossRef]
26. *ASTM D3801-20a*; Standard Test Method for Measuring the Comparative Burning Characteristics of Solid Plastics in a Vertical Position. ASTM: West Conshohocken, PA, USA, 2020.
27. *ASTM D2863-23*; Standard Test Method for Measuring the Minimum Oxygen Concentration to Support Candle-like Combustion of Plastics (Oxygen Index). ASTM: West Conshohocken, PA, USA, 2023.
28. *ISO 5660-1:2015*; Reaction-to-Fire Tests—Heat Release, Smoke Production and Mass Loss Rate—Part 1: Heat Release Rate (Cone Calorimeter Method) and Smoke Production Rate (Dynamic Measurement). ISO: Geneva, Switzerland, 2015.
29. Neisius, N.M.; Lutz, M.; Rentsch, D.; Hemberger, P.; Gaan, S. Synthesis of DOPO-based phosphonamiDTAes and their thermal properties. *Ind. Eng. Chem. Res.* **2014**, *53*, 2889–2896. [CrossRef]
30. Chen, Y.K.; Lu, Q.X.; Zhong, G.; Zhang, H.G.; Chen, M.F.; Liu, C.P. DOPO-based curing flame retardant of epoxy composite material for char formation and intumescent flame retardance. *J. Appl. Polym. Sci.* **2021**, *138*, 49918. [CrossRef]
31. Huo, S.Q.; Wang, J.; Yang, S.; Chen, X.; Zhang, B.; Wu, Q. Flame-retardant performance and mechanism of epoxy thermosets modified with a novel reactive flame retardant containing phosphorus, nitrogen, and sulfur. *Polym. Adv. Technol.* **2018**, *29*, 497–506. [CrossRef]
32. Deng, P.; Liu, Y.S.; Liu, Y.; Xu, C.G.; Wang, Q. Preparation of phosphorus-containing phenolic resin and its application in epoxy resin as a curing agent and flame retardant. *Polym. Adv. Technol.* **2018**, *29*, 1294–1302. [CrossRef]
33. Yang, J.W.; Wang, Z.Z. Thermal and flame retardant properties of epoxy resin cured by a novel phosphorus-containing 4, 4′-bisphenol novolac curing agent. *Phosphorus Sulfur Silicon Relat. Elem.* **2017**, *192*, 1294–1300. [CrossRef]
34. Zilberman, J.; Yoffe, D.; Piotrowski, A.; Singh, M.P.; Suryadevara, K.; Levchik, S. Comparative study of reactive flame retardants based on 9, 10-dihydro-9-oxa-10-phosphaphenanthrene 10-oxide. *J. Fire Sci.* **2017**, *35*, 235–256. [CrossRef]
35. Sag, J.; Goedderz, D.; Kukla, P.; Greiner, L.; Schönberger, F.; Döring, M. Phosphorus-containing flame retardants from biobased chemicals and their application in polyesters and epoxy resins. *Molecules* **2019**, *24*, 3746. [CrossRef] [PubMed]
36. Wu, H.Y.; Hu, R.; Zeng, B.R.; Yang, L.; Chen, T.; Zheng, W.; Liu, X.; Luo, W.; Dai, L. Synthesis and application of aminophenyl-s-triazine derivatives as potential flame retardants in the modification of epoxy resins. *RSC Adv.* **2018**, *8*, 37631–37642. [CrossRef] [PubMed]
37. Xu, Y.J.; Chen, L.; Rao, W.H.; Qi, M.; Guo, D.M.; Liao, W.; Wang, Y.Z. Latent curing epoxy system with excellent thermal stability, flame retardance and dielectric property. *Chem. Eng. J.* **2018**, *347*, 223–232. [CrossRef]
38. Liu, X.D.; Zheng, X.T.; Dong, Y.Q.; He, L.X.; Chen, F.; Bai, W.B.; Lin, Y.C.; Jian, R.K. A novel nitrogen-rich phosphinic amide towards flame-retardant, smoke suppression and mechanically strengthened epoxy resins. *Polym. Degrad. Stab.* **2022**, *196*, 109840. [CrossRef]
39. Li, S.N.; Zhao, X.J.; Liu, X.H.; Yang, X.; Yu, R.; Zhang, Y.; Huang, W.; Deng, K. Cage-ladder-structure, phosphorus-containing polyhedral oligomeric silsesquinoxanes as promising reactive-type flame retardants for epoxy resin. *J. Appl. Polym. Sci.* **2019**, *136*, 47607. [CrossRef]
40. Szołyga, M.; Dutkiewicz, M.; Nowicki, M.; Salasinska, K.; Celinski, M.; Marciniec, B. Phosphorus-Containing Silsesquioxane Derivatives as Additive or Reactive Components of Epoxy Resins. *Materials* **2020**, *13*, 5373. [CrossRef]
41. Huo, S.Q.; Liu, Z.T.; Li, C.; Wang, X.L.; Cai, H.P.; Wang, J. Synthesis of a phosphaphenanthrene/benzimidazole-based curing agent and its application in flame-retardant epoxy resin. *Polym. Degrad. Stab.* **2019**, *163*, 100–109. [CrossRef]
42. Chai, H.Y.; Li, W.X.; Wan, S.B.; Liu, Z.; Zhang, Y.F.; Zhang, J.H.; Kong, Q.H. Amino Phenyl Copper Phosphate-Bridged Reactive Phosphaphenanthrene to Intensify Fire Safety of Epoxy Resins. *Molecules* **2023**, *28*, 623. [CrossRef]
43. Hamciuc, C.; Serbezeanu, D.; Carja, I.D.; Vlad-Bubulac, T.; Musteata, V.E.; Forrat Pérez, V.; Guillem López, C.; López Buendia, A.M. Effect of DOPO units and of polydimethylsiloxane segments on the properties of epoxy resins. *J. Mater. Sci.* **2013**, *48*, 8520–8529. [CrossRef]
44. Hamciuc, C.; Vlad-Bubulac, T.; Serbezeanu, D.; Carja, I.D.; Hamciuc, E.; Lisa, G.; Pérez, V.F. Environmentally friendly fire-resistant epoxy resins based on a new oligophosphonate with high flame retardant efficiency. *RSC Adv.* **2016**, *6*, 22764–22776. [CrossRef]

45. Wang, R.Z.; Chen, Y.; Liu, Y.Y.; Ma, M.L.; Hou, Y.B.; Chen, X.; Ma, Y.; Huang, W. Synthesis of sugar gourd-like metal organic framework-derived hollow nanocages nickel molybDTAe@cobalt-nickel layered double hydroxide for flame retardant polyurea. *J. Colloid Interface Sci.* **2022**, *616*, 234–245. [CrossRef] [PubMed]
46. Kong, Q.H.; Zhu, H.J.; Huang, S.; Wu, T.; Zhu, F.; Zhang, Y.L.; Wang, Y.; Zhang, J.H. Influence of multiply modified FeCu-montmorillonite on fire safety and mechanical performances of epoxy resin nanocomposites. *Themochim. Acta* **2022**, *707*, 179112. [CrossRef]